Electronic Supplementary Material (ESI) for Green Chemistry.
This journal is © The Royal Society of Chemistry 2020

Supporting information for:

Self-repairing microcapsules with aqueous solutions as core materials for conductive applications

Furong Li[a], Shouzheng Jiao[a], Zhicheng Sun* [a], Yuanyuan Liu[b], Qingqing Zhang[a], Jinyue Wen[a], Yang Zhou*[b]

[a] Beijing Engineering Research Center of Printed Electronics, School of Printing and Packaging Engineering, Beijing Institute of Graphic Communication, 102600, Beijing, China

E-mail: sunzhicheng@bigc.edu.cn

[b] Key Laboratory of Advanced Materials of Tropical Island Resources of Ministry of Education and School of Chemical Engineering and Technology, Hainan University Haikou, Hainan 570228, China
E-mail: yzhou@hainanu.edu.cn

1. Experimental details

1.1. Materials

All the chemicals were purchased and directly used without any purification. Liquid paraffin, sodium dodecyl sulfate (SDS), Tianjin Guangfu Fine Chemical Research Institute. Span-80, Fe_3O_4 dispersion (Fe_3O_4, 25% dispersion solution), anhydrous citric acid, Shanghai Aladdin Biochemical Technology Co., Ltd.. Triethanolamine (AR), Sinopharm Chemical Reagent Co., Ltd.. Melamine (>99%), McLean Chemical Reagent Co., Ltd.. Formaldehyde (37% aqueous solution), Braunwell Technology Co., Ltd.. Ammonium persulfate $(NH_4)_2S_2O_8$, Beijing Chemical Plant. Calcium stearate, Tishila (Shanghai) Chemical Industry Development Co., Ltd.. Poly 3,4-ethylenedioxythiophene/ polystyrenesulfonate solution (PEDOT: PSS), Heraeus Konzern. Single Layer Graphene Dispersion (GR), Graphene Labs.

1.2. Synthesis of self-repairing microcapsules with conductive aqueous solution

1) A mixture of conductive aqueous solution (such as PEDOT:PSS water solution, Graphene dispersed aqueous solution, Fe_3O_4 dispersed aqueous solution, Running water, Deionized water), $(NH_4)_2S_2O_8$, and SDS was initially added into a beaker (100 mL) with a mass ratio of 25: 2.5: 1 as shown in Table S1. The mixed-solution was magnetically stirred for 30 min to get a core material solution.

2) A mixture of formaldehyde (5.15 g 37% aqueous solution) and melamine (2.35 g) was dissolved in water (19.5 g). Then the pH of the solution was adjusted to 8-9 by using 10% triethanolamine aqueous solution. The above solution was kept at 500 rpm and 70 ^{o}C for 30 min to obtain the melamine-formaldehyde prepolymer solution.

3) A mixture of liquid paraffin (50 g), Span-80 (1.5 g), and calcium stearate (0.05 g) were prepared in a 250 mL flask. The solution was mechanically stirred at 70 ^{o}C for 60 minutes to obtain the organic solvent.

4) Subsequently, a stable W/O emulsion was obtained with a rapid stirring over 10 min by using the core material solution (14.25 g), the melamine-formaldehyde prepolymer solution (27 g) and the organic solvent (51.55 g). The resulting emulsion was further placed at 70 ^{o}C and 500 rpm for 3.5 hours to obtain crude self-healing microcapsule products. The crude product was centrifuged, washed, and vacuum dried at 50 ^{o}C to obtain self-repairing microcapsules.

Table S1. The composition of conductive aqueous microcapsules

Conductive aqueous microcapsules				
Core	Conductive aqueous solution		(a)PEDOT: PSS water solution(g)	12.5
			(b) Graphene dispersed aqueous solution(g)	12.5
			(c)Fe_3O_4 dispersed aqueous solution(g)	12.5
			(d)Running water (g)	12.5
			(e)Deionized water (g)	12.5
	$(NH_4)_2S_2O_8$(g)	1.25		
	SDS(g)	0.5		
Shell	Formaldehyde(g)	2.35		
	Melamine(g)	5.15		
	Water(g)	19.5		
Organic solvents	Paraffin(g)	50		
	Span-80(g)	1.5		
	Calcium stearate(g)	0.05		

1.3. Characterization

The surface morphology of dried microspheres was observed by scanning electron microscopy (SEM, SU8020, HITACHI, Japan) under vacuum conditions with a voltage of 3 kV. The absorption spectrum of microspheres was obtained by Fourier transform infrared spectroscopy (FTIR, NICOLET IS10, Thermo Fisher Scientific) with a scanning range of 4000 cm^{-1}-500 cm^{-1}, and the scanning time was 32 times. The particle size distribution of the microcapsules was measured with a Mastersizer 2000 laser particle size analyzer (Mastersizer 2000, Malvern Instruments Ltd.). During the measurement, the microcapsule sample was uniformly dispersed in ethanol. The phase change latent heat of the samples was analyzed by differential scanning calorimeter (DSC, DSC214, NETZSCH Technology Company, Germany). The sample was placed in a nitrogen atmosphere to determine the phase transition characteristics of the dried microcapsules under the heating / cooling (10 ^{o}C / min). The temperature was ranged from 0 ^{o}C to 200 ^{o}C during the test. The thermal stability of microcapsules was evaluated by using a thermogravimetric analyzer (TG, TG209F3, NETZSCH Technology Company, Germany). In each measurement, the temperature of sample in a nitrogen atmosphere raised from 30 ^{o}C to 800 ^{o}C with a scan rate of 20 ^{o}C/min. The weight loss was used to indicate the thermal stability of the sample. The compressive strength of microcapsules was analyzed by using a compressive strength machine (Xin Sansi compressive strength machine). The sample (30 mg) was loaded into a sample tank, and was slightly shaken to obtain a solid microcapsule stack. The upper and lower pole plates were statically pressed with a speed of 1 mm / min, until the capsule was completely broken. The conductivity of the microcapsule core material was measured by using a conductivity meter.

2. Surface morphology of PEDOT: PSS microcapsules with different core-wall ratio

It can be seen from the SEM pictures that the microcapsules with different core-to-wall ratios have spherical structures and relatively uniform size. In addition, it can be observed from the SEM pictures that the surface of the microcapsules gradually becomes smooth with the increase of core material content. Because the prepolymer is slightly soluble in water and the solubility of the prepolymer may gradually increase as the content of the core material increases. Therefore, the resin particles generated by the prepolymer reaction become more uniform, which results in a smoother surface of the microcapsules.

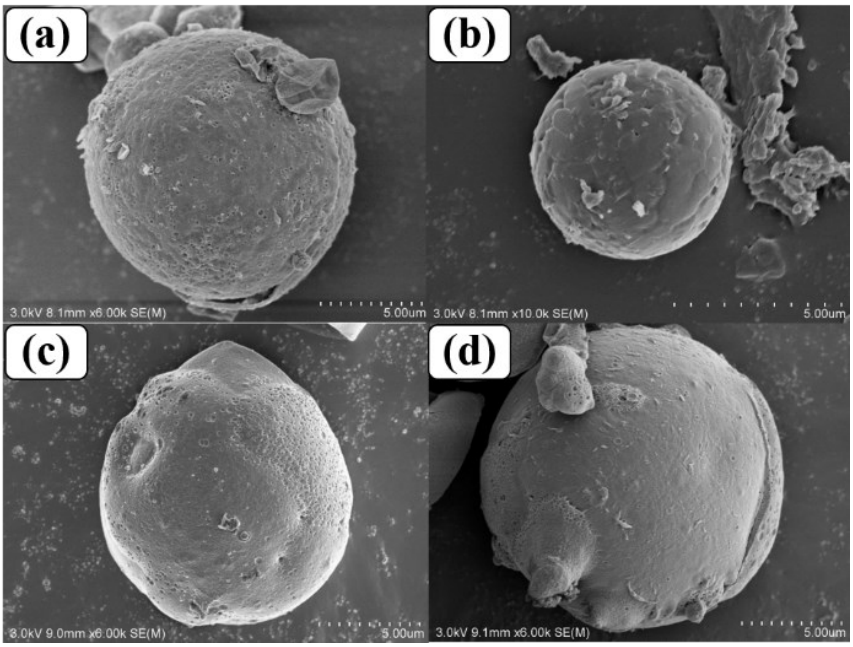

Figure S1. SEM images of PEDOT: PSS microcapsules with different core-wall ratios

Note: (a) PEDOT: PSS microcapsule with a core-to-wall ratio of 1: 1, (b) PEDOT: PSS microcapsule with a core-to-wall ratio of 1.5: 1, (c) PEDOT: PSS microcapsules with a core-to-wall ratio of 2: 1, (d) PEDOT: PSS microcapsule with a core-to-wall ratio of 3: 1.

3. Thermogravimetric distribution of PEDOT: PSS microcapsules with different core-wall ratios

According to the DSC curves of Figure S2-a and Figure S2-b, the phase change latent heat of the PEDOT:PSS aqueous microcapsules with different core-wall ratios was different. The figure illustrated that the latent heat of phase change of the microcapsules with different core-wall ratios was from small to large: 1:1, 1.5:1, 3:1, 2:1.

It can be seen from Figure S2-c that although the decomposition curves of PEDOT: PSS microcapsules with different core-to-wall ratios are similar, the decomposition rates are different. The decomposition of microcapsules is mainly divided into two parts, one is the decomposition of the core material, and the other is the decomposition of the wall material. The core materials of the microcapsules began to decompose at 20 ^{o}C. When the temperature reaches about 200 ^{o}C, the internal pressure of the microcapsules reaches a maximum. As heat continue, the microcapsules burst, the core material escapes quickly, and the microcapsules lose weight quickly. When the temperature reaches about 440 ^{o}C, the microcapsule wall material decomposition temperature is reached. When the temperature rises to about 800 ^{o}C, most of the wall material of the microcapsules will be completely decomposed. Due to the varied contents of the core material, the decomposition rate of the

microcapsules was also different. According to Figure S2-d, the smaller the core material content, the slower the decomposition rate of the microcapsules would be. The decomposition rate of the microcapsules was from large to small: 2:1, 3:1, 1.5:1, 1:1.

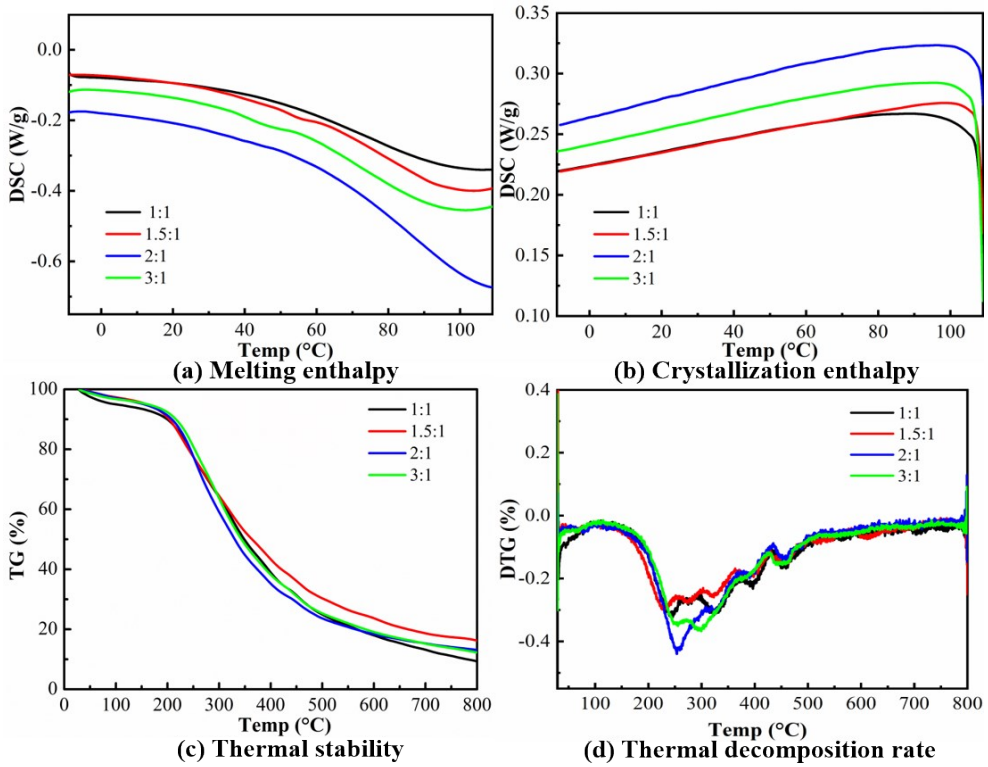

Figure S2. Thermogravimetric curves of PEDOT: PSS microcapsules with different core-wall ratios

4. Bearing pressure analysis of PEDOT: PSS microcapsules with different core-wall ratios

It can be seen from the pressure curve that although the pressure curves of the microcapsules with different core-wall ratios are similar, the pressure-bearing capabilities of the microcapsules with different core-wall ratios are different. According to Table S2, it can be seen that the smaller the core-wall ratio, the greater the microcapsule's initial pressure-bearing capacity. This is because the smaller the core-wall ratio, the smaller the particle size of the microcapsules will be. The smaller the particle size of the microcapsules, the larger the gap between the microcapsules. Therefore, the initial pressure of the microcapsules is greater. However, the maximum pressure at which all the microcapsules were crushed is directly proportional to the particle size of the microcapsules and the core-to-wall ratio of the microcapsules. The more the microcapsules cover the core material, the greater the microcapsule's ability to withstand pressure.

Table S2. Pressure bearing capacity of PEDOT: PSS microcapsules with different core-wall ratios

Type	Start to crack (N)	All rupture (N)
1:1	12.55	14.00
1.5:1	12.31	14.24
2:1	12.06	15.20
3:1	11.58	14.48

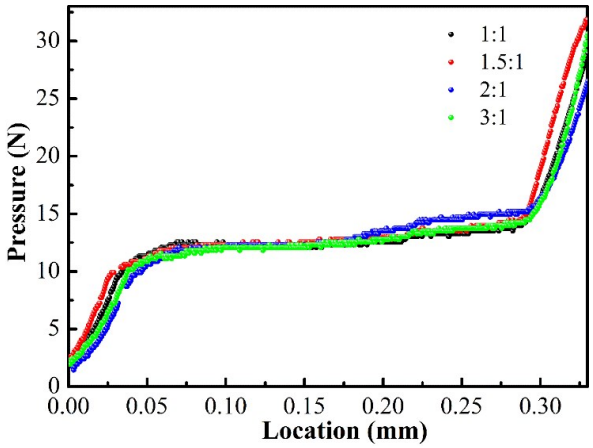

Figure S3. Bearing pressure curves of PEDOT: PSS microcapsules with different core-wall ratios

5. Surface morphology of microcapsules with different core materials

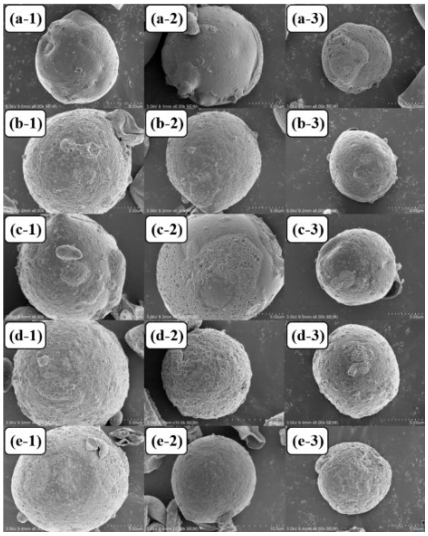

Figure S4. Surface morphology of microcapsules with different core materials

Note: (a) MC1, (b) MC2, (c) MC3, (d) MC4, (e) MC5.

6. Fractured surface morphology of microcapsules with different core materials

In order to quantify the shell thickness of the microcapsules, we ruptured the microcapsules using pressure. The shell thickness of the cracked microcapsules will be observed by SEM. We randomly selected dozens of microcapsules from different kinds of microcapsules for the statistical analysis of shell thickness of these microcapsules. As shown in Table S3 and Figure S5, the average thickness of the MC1 shell was determined to be ~0.65 μm, the MC2 shell thickness was ~0.73 μm, the MC3 shell thickness was ~1.32 μm, the MC4 shell thickness was ~0.34 μm, and the MC5 shell thickness was ~0.25 μm. In addition, it can be seen from Table S3 that the thicknesses of the microcapsules were different for different microcapsules and cross sections.

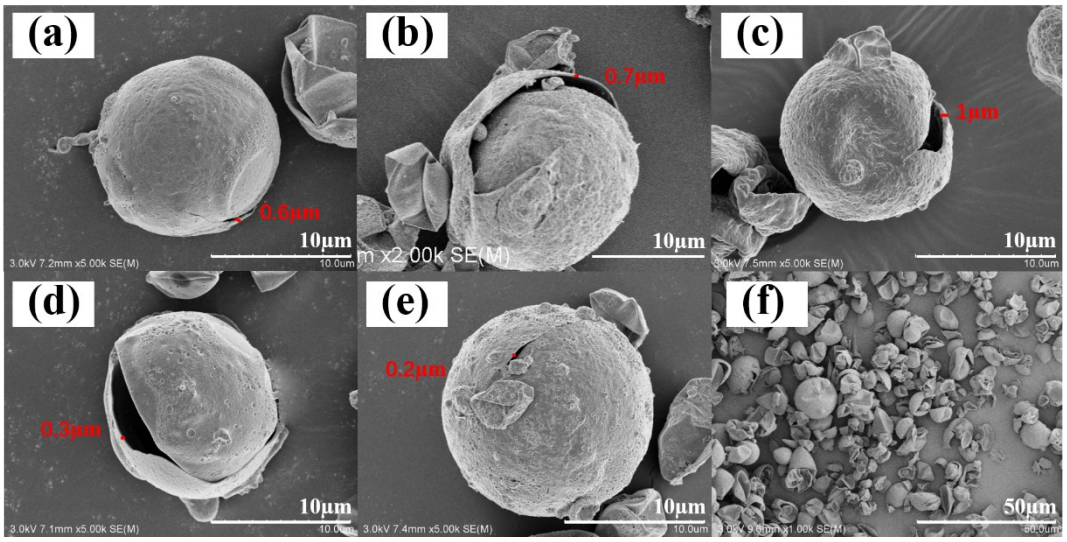

Figure S5. Fractured surface morphology of microcapsules with different core materials

Note: (a) MC1, (b) MC2, (c) MC3, (d) MC4, (e) MC5, (f) Cracked MC1 microcapsules.

Table S3. Shell thickness of different conductive aqueous microcapsules

Type	MC1	MC2	MC3	MC4	MC5
First (μm)	0.47	0.50	0.80	0.24	0.16
Second (μm)	0.54	0.67	1.00	0.26	0.17
Third (μm)	0.60	0.70	1.29	0.30	0.20
Fourth (μm)	0.79	0.87	1.68	0.41	0.35
Fifth (μm)	0.85	0.91	1.83	0.49	0.37
Average (μm)	0.65±0.20	0.73±0.23	1.32±0.51	0.34±0.15	0.25±0.12

7. Conductivity of different core materials

Table S4. Conductivity(σ) of different core materials

Type	First	Second	Third	Fourth	Fifth	Average
MC1(ms/cm)	6.210	6.240	6.210	6.270	6.230	6.232
MC2(ms/cm)	1.881	1.879	1.881	1.880	1.879	1.880
MC3(ms/cm)	3.040	3.080	2.959	3.041	3.027	3.029
MC4(ms/cm)	0.715	0.705	0.732	0.757	0.735	0.729
MC5(ms/cm)	1.430	1.401	1.432	1.410	1.460	1.427

Note: MC1 is PEDOT: PSS aqueous solution microcapsules, MC2 is graphene dispersion aqueous microcapsules, MC3 is Fe_3O_4 dispersion aqueous microcapsules, MC4 is running water microcapsules, MC5 is deionized water microcapsules.

8. Mechanism of self-repairing microcapsules repaired conductive circuit

During the practical applications, conductive self-repairing microcapsules were widely attached to the surface of electronic equipment or wires. Due to the long-term power consumption, the equipment would generate a large amount of heat to reduce the efficiency of the machine. Using the conductive self-repairing microcapsules attached to the device, in contrast, the heat generated by the device would be effectively absorbed, which can prevent the overheating of the device itself, and maintain the high operation efficiency. In particular, when the device was damaged, pressing the damaged part of the device would release the conductive solution from microcapsules into the damaged part, resulting in the self-repairing of the short circuit of the device (see Figure S6).

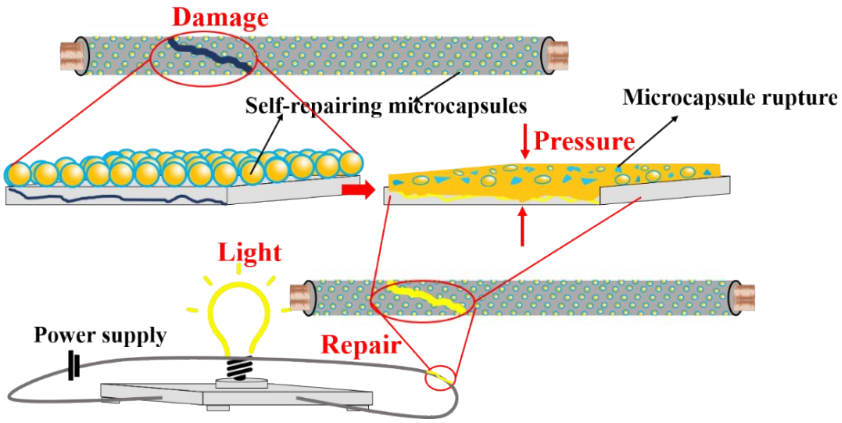

Figure S6. The possible working principle of self-repairing microcapsules for conductive aqueous solution

9. Repair effect of conductive particles

We freeze-dried the conductive aqueous solution (PEDOT:PSS, graphene solution, Fe_3O_4 solution) to obtain pure conductive particles, which were used to repair damaged circuits. When the conductive particles were directly injected into the damaged part of the copper foil, it was found that the damaged part had not been repaired, as shown in Figure S7. It is likely that the gaps between pure conductive particles were too large, therefore, electronic transmission between conductive particles cannot be achieved. In addition, pure conductive particles cannot also repair the subtle parts and deep parts of the damaged circuit due to the lack of mobility and electronic transmission. Therefore, only the conductive core material in the form of an aqueous solution can have the fluidity and the conductivity.

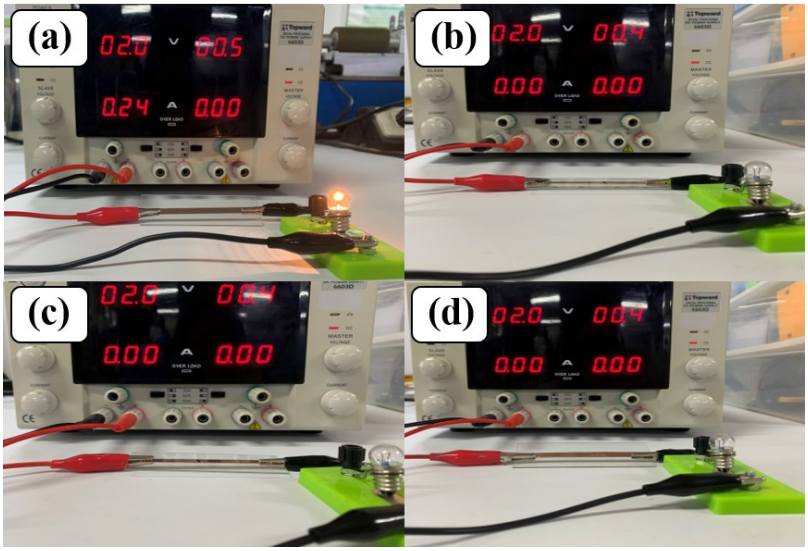

Figure S7. Repair effect of conductive particles

Note: (a) the copper foil under normal operation, (b) PEDOT:PSS, (c) Graphene, (d) Fe_3O_4.

10. Thermal stability curve of melamine-formaldehyde resin

According to the research of S. Ullah's team[1] and B. Friedel's team[2], it could be seen that the melamine-formaldehyde resin produced methanol, formaldehyde, amine and other gases during the process of heating from 400 °C to 800 °C. Therefore, according to Figure S8, it could be seen that when the temperature of the pure melamine-formaldehyde resin reached 800°C, the remaining undecomposed material of melamine-formaldehyde resin should be the carbonized residue. The mass of the melamine-formaldehyde resin residue was about 20%, based on the calculation through the following formula (5).

$$R_r = \frac{M_r}{M_e} \times 100\% \quad (5)$$

Where M_r referred to the weight of the melamine-formaldehyde resin carbonized residue, M_e referred to the weight of the total melamine-formaldehyde resin, R_r referred to the percentage of carbonized residue of resin.

Figure 4-a showed the weight of the melamine-formaldehyde resin carbonized residue and conductive particles in the microcapsules when the temperature of the microcapsules reached up to 800 °C. The remaining total mass was about 15% according to the calculation formula (6).

$$R_m = \frac{M_r + M_c}{M_m} \times 100\% \quad (6)$$

Where M_r referred to the weight of the melamine-formaldehyde resin carbonized residue in the microcapsules, M_c referred to the weight of the conductive particles in the microcapsules, and M_m referred to the weight of the microcapsules, R_m referred to the percentage of the remaining weight.

The above results represented the thermodynamic stability of two different materials, so the percentages of the remaining weight of the two materials are not comparable.

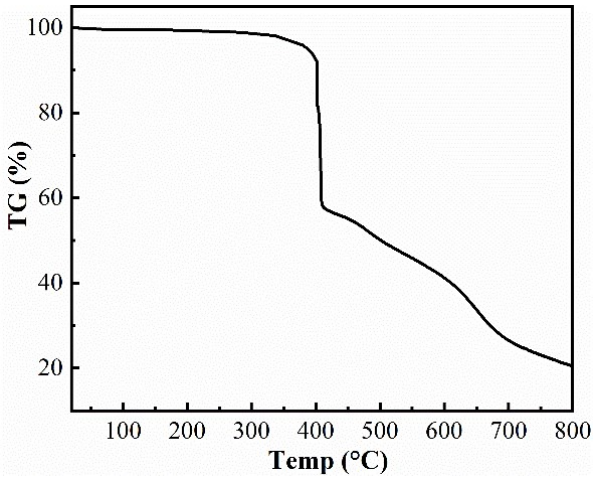

Figure S8. Thermal stability curve of melamine-formaldehyde resin

11. DSC of conductive particles

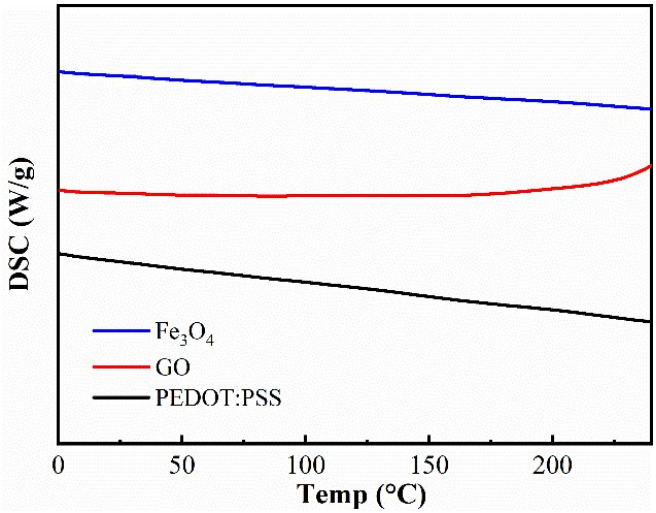

Figure S9. Latent heat of phase change of conductive particles

According to Figure S9, it could be seen that PEDOT:PSS, graphene and ferroferric oxide had good thermal stability[3,4].

12. Loading rate of microcapsules

According to TG results, the quality of water in the microcapsule core material can be calculated. According to the calculation formula of conductive aqueous solution (7), the quality of conductive particles in the microcapsule core material can be obtained.

$$C_c = \frac{M_c}{M_w + M_c} \times 100\% \quad (7)$$

Where M_c was the weight of conductive particles, M_w was the weight of water, and M_c was the concentration of conductive particles.

In the formula of microcapsule loading rate (8), the loading rate of different microcapsules can be determined.

$$L = \frac{M_w + M_C}{M_m} \times 100\% \quad (8)$$

Where M_C was the weight of the conductive particles, M_w was the weight of water, M_m was the weight of the microcapsules, and L was the loading rate of the microcapsules.

Using the equation 7, the loading rate of MC1, MC2, MC3, MC4, MC5 was determined to be 75.329%, 85.190%, 84.003%, 85.812%, and 86.334%, respectively. Since the shell began decompose after 400 ^{o}C, the decomposition of the shell was not related to the calculation of the loading rate.

13. The effect of core-wall ratio on shell

The core-to-wall ratio was achieved by increasing or decreasing the quality of the core material under the condition that the quality of the wall material remained unchanged. As the quality of the core material increased, the volume of emulsified droplets will gradually increase. As the volume of the droplet increases, the surface area of the droplet will increase. Since the quality of the wall material was a fixed value, as the surface area of the droplet increases, the thickness of the wall material attached to the surface of the droplet will decrease. Therefore, the shell thickness of the microcapsule can be changed by controlling the core-wall ratio.

14. Advantages of conductive aqueous solution self-repairing microcapsules

The current microcapsule self-healing technology only includes metal [5,6] and carbon materials [7,8,9] as two kinds of repairing agents as core materials. However, liquid metal materials were costly. Organic solvents used as carbon materials were volatile and toxic. Therefore, the development of inexpensive and green microcapsules would be of significant interest to promote the sustainability of self-repairing agents in the electronic device area. The self-repairing microcapsules prepared in this work have three functions: environmental protection, repairing, and cooling. The environmental protection function was that the liquid paraffin, a conductive aqueous solution and melamine-formaldehyde resin were employed as the organic solvents, core material, and shell layer, respectively. All the preparation materials and processes were completely green, non-toxic and non-polluting. The repair function was to attach the self-healing microcapsule to the surface of the electronic circuit. When the circuit was damaged, the microcapsule was crushed by the pressure to release the conductive solution on the damaged part. In this way, the electronic device can restore its conductivity within a few seconds. The cooling function was that the microcapsule core material had phase change latent heat, which can reduce the temperature of the circuit itself during long-term operation of the circuit and maintain the efficient operation of the device.

Notes and references

[1] S. Ullah, M. A.Bustam, M. Nadeem, M. Y. Naz, W. L. Tan, A. M. Shariff, *The Scientific World Journal*, 2014.

[2] B. Friedel, S. Greulich-Weber, *small*, 2006, **2**, 859.

[3] H. Shi, C. Liu, Q. Jiang, J. Xu, *Adv. Electron. Mater.* 2015, **1**, 1500017.

[4] S. Ayyappan, G. Gnanaprakash, G. Panneerselvam, M. P. Antony, J. Philip, *J. Phys. Chem.*

C, 2008, **112**, 18376.

[5] K. Chu, B. G. Song, H. I. Yang, D. M. Kim, C. S. Lee, M. Park, C. M. Chung, *Adv. Funct. Mater*, 2018, **28**, 1800110.

[6] B. J. Blaiszik, S. L. B. Kramer, M. E. Grady, D. A. Mcllroy, J. S. Moore, N. R. Sottos, S. R. White, *Adv. Mater*, 2012, **24**, 398.

[7] S. A. Odom, T. P. Tyler, M. M. Caruso, J. A. Ritchey, M. V. Schulmerich, S. J. Robinson, R. Bhargava, N. R. Sottos, S. R. White, M. C. Hersam, J. S. Moore, *Appl. Phys. Lett*, 2012, **101**, 043106.

[8] M. M. Caruso, S. R. Schelkopf, A. C. Jackson, A. M. Landry, P. V. Braun, J. S. Moore, *J. Mater. Chem*, 2009, **19**, 6093.

[9] H. H. Zamal, D. Barba, B. Aïssa, E. Haddad, F. Rosei, *Sci Rep*, 2020, **10**, 1.